



# The Mechanism of Cu<sup>2+</sup> Sorption by Rice Straw Biochar and Its Sorption–Desorption Capacity to Cu<sup>2+</sup> in Soil

Xiaobing Wang<sup>1,2</sup> · Shuai Ma<sup>1</sup> · Xiaoli Wang<sup>1</sup> · Tong Cheng<sup>1</sup> · Junneng Dong<sup>1</sup> · Ke Feng<sup>1,2</sup>

Received: 31 August 2021 / Accepted: 19 April 2022 / Published online: 3 June 2022  
© The Author(s), under exclusive licence to Springer Science+Business Media, LLC, part of Springer Nature 2022

## Abstract

Copper (Cu) pollution in soils has received considerable research attention globally, and biochar has been widely used as an adsorbent for soil pollution of Cu. However, most of the studies focused on the adsorption capacity of biochar, the bioavailability of Cu adsorbed by biochar remains unclear. In this work, rice straw biomass was pyrolyzed under oxygen-limited conditions at 400°C (BC400) and 600°C (BC600), their apparent structure, group characteristics, and basic physical and chemical properties were determined. The isothermal and kinetics adsorption of Cu by BC400 and BC600 were analyzed. A pot experiment was used to evaluate the passivation of Cu in the soil by biochar and the bioavailability of Cu adsorbed by biochar in the soil. The smooth surfaces of BC400 evolved into more rough surfaces for BC600, and both types of surfaces may give active sorption sites for Cu, according to SEM pictures. FTIR analysis suggested that BC600 is endowed with more condensed aromatic carbon structures and more available polar functional groups. The adsorption processes of Cu<sup>2+</sup> by biochar were better fitted Langmuir equation and pseudo-second-order kinetic model. The adsorption isotherms showed monolayer adsorption of Cu<sup>2+</sup> on biochar. The maximum adsorption capacities of BC600 and BC400 on Cu<sup>2+</sup> were 43.75 and 30.70 mg g<sup>-1</sup>, respectively. Moreover, the pot experiment showed that BC400 and BC600 not only have a strong “passivation” effect on Cu in soil but also prevent the release of adsorbed Cu. Overall, more aromatic carbon structure, more polar functional groups, and higher pH are associated with BC600’s increased Cu immobilization ability in soil.

**Keywords** Rice straw biochar · Copper · Structural characterization · Adsorption · Bioconcentration factor

Copper (Cu) is an essential mineral element for plant growth, but it is toxic to plants and animals, including humans when the concentration of copper reaches or exceeds a certain level (Kim et al. 2020; Rakhra et al. 2017; Shahid et al. 2016). At present, the remediation measures of heavy metal pollution mainly include physical (Yuvaraj et al. 2021), chemical remediation (Rambabu et al. 2019), and biological remediation (Akcil et al. 2015; Ndeddy Aka and Babalola 2016). Biochar has the ability to adsorb and passivate heavy metals in soil, which can be used as a remediation approach for heavy metal contaminated soil (Li et al. 2019; Namgay et al. 2010). Possible mechanisms for biochars contributed to the heavy metal immobilization were

precipitation and adsorption (primarily electrostatic interactions, ionic exchange, and complexation) of metal ions on biochars (Salam et al. 2019; Uchimiya et al. 2011) which is due to its large surface area, high porosity and pH, and a large number of active functional groups such as hydroxyl, carboxyl and carbonyl groups (He et al. 2018; Rizwan et al. 2020).

During the process of producing biochar by straw, major researches focus on the passivation of biochar on heavy metals in soil (Chen et al. 2020). However, it’s unclear whether the heavy metals absorbed by biochar are released again. In this study, two kinds of rice straw biochar were prepared at 400°C (BC400) and 600°C (BC600). Their apparent structure, group characteristics, and basic physical and chemical properties were determined. The isothermal adsorption and kinetics adsorption of Cu were analyzed. The biological effects of BC400 and BC600 on the passivation of Cu in the soil were evaluated by a pot experiment. The objectives of this study were to determine the following:(1) the adsorption efficiency to Cu by rice straw biochar prepared at different

✉ Xiaobing Wang  
xbwangll@hotmail.com

<sup>1</sup> College of Environmental Science and Engineering,  
Yangzhou University, Yangzhou 225127, China

<sup>2</sup> Jiangsu Collaborative Innovation Center for Solid Organic  
Waste Resource Utilization, Nanjing 210095, China

temperatures; (2) the effect of Copper-loaded biochar on the chemical morphology of copper ions in soil; (3) determine the passivation and sorption–desorption capacity of biochar to  $\text{Cu}^{2+}$  in soil.

## Materials and Methods

Rice straw, collected from Hai'an, Jiangsu province, China ( $120^\circ 22' \text{ E}$ ,  $32^\circ 22' \text{ N}$ ), was washed three times in deionized water and dried at  $75^\circ\text{C}$  for 48 h, then crushed to pass through a 0.90-mm sieve. The rice straw has the following properties: pH 6.18, nitrogen  $6.12 \text{ g kg}^{-1}$ , phosphorus  $3.52 \text{ g kg}^{-1}$  and potassium  $12.71 \text{ g kg}^{-1}$ , Cu  $5.65 \text{ mg kg}^{-1}$ . The rice straw was subjected to oxygen-limited cracking, in which it was placed in a rectangular corundum porcelain boat and pyrolyzed in a tube-furnace under  $\text{N}_2$  protection. The pyrolysis temperature was set between  $400$  and  $600^\circ\text{C}$  with a heating rate of  $10^\circ\text{C min}^{-1}$  and held at the peak temperature for 4 h. When the biochar had cooled to room temperature ( $25^\circ\text{C}$ ), it was collected, weighed, and crushed to pass through a 0.15-mm sieve. The BC400 and BC600 were then stored for compositional analysis.

The ash content of biochars was determined by burning method, a small amount of biochar placed in the muffle furnace and burned at  $750^\circ\text{C}$  for 6 h (Brewer et al. 2014) and the pH of biochar was determined in deionized water at the ratio of 1:2.5 (*m:v*) with a pH meter (Inesa Inc., Shanghai, China).

The  $\text{pH}_{\text{pzc}}$  for biochar were determined by the following procedure (Medellin-Castillo et al. 2007): 25 mL of  $0.1 \text{ mol L}^{-1} \text{ KNO}_3$  solution was added to a 50-mL centrifugal tube and bubbled with nitrogen gas to expel dissolved  $\text{CO}_2$ . Next, 0.500 g biochar was added,  $0.1 \text{ mol L}^{-1} \text{ HNO}_3$  or  $0.1 \text{ mol L}^{-1} \text{ NaOH}$  were used to adjust the solution pH to a selected value from 2 to 12, then the samples were shaken at 160 rpm for 24 h at room temperature. Then the samples were filtrated and the final pH was measured separately, the pH difference ( $\Delta\text{pH}$ ) between final pH ( $\text{pH}_f$ ) and initial pH ( $\text{pH}_i$ ) was plotted against the initial pH ( $\text{pH}_i$ ), the point at which  $\Delta\text{pH}$  equal to zero was considered to be the  $\text{pH}_{\text{pzc}}$ .

Different biochar materials were scanned by S-4800II field emission scanning electron microscopy (FESEM, HITACHI, Japan) to observe the microstructure and morphology; the elements of biochar were determined by energy dispersive spectroscopy (Arakaki et al. 2006) and Vario EL cube element analyzer (Elementar Analysensystem, GmbH, Germany), the specific surface area of biochar was determined by Autosorb IQ3 specific surface area and pore size were measured based on the Brunauer-Emmet-Teller (BET) (Autosorb IQ3, Quantachrome, USA).

To study adsorption isotherms, 0.30 g of biochar received 50 mL of  $\text{CuSO}_4$  solution with  $\text{Cu}^{2+}$  concentration of

$200 \text{ mg L}^{-1}$ , and samples were collected at 0, 3 min, 12 min, 30 min, 1 h, 2 h, 4 h, 6 h, 8 h, 12 h, 16 and 20 h. The sample was shaken for 24 h on a shaker at  $200 \text{ r min}^{-1}$  and  $25^\circ\text{C}$ , and then filtered through a  $0.45 \mu\text{m} \times 150 \text{ mm}$  filter. The concentration of heavy metals in the filtrate was determined with an inductively coupled plasma mass spectrometer (ICP-MS; Thermo Fisher Scientific, USA). The amount of heavy metal adsorbed by the biochar was calculated according to the change of the heavy metal content in the solution before and after the treatment. The initial pH value of the mixtures was adjusted to  $5.5 \pm 0.05$  using HCl and NaOH solution ( $0.1 \text{ M}$ ) under stirring. All tests were conducted in triplicate. The experiment was conducted at room temperature ( $25^\circ\text{C}$ ).

To investigate the adsorption characteristics of Cu by biochar prepared at different temperatures, the Langmuir and Freundlich isotherm adsorption equations for Cu adsorption were fitted (Haghtalab et al. 2012). The formulas are as follows:

$$\text{Langmuir adsorption isotherm is : } q_e = \frac{Kq_m C_e}{1 + KC_e}$$

$$\text{Freundlich adsorption isotherm can be expressed as : } q_e = K_f C_e^{1/n}$$

where  $q_e$  represents the amount of adsorption at equilibrium ( $\text{mg/g}$ );  $C_e$  represents the solution concentration at equilibrium ( $\text{mg L}^{-1}$ );  $q_m$  represents the maximum adsorption capacity ( $\text{mg g}^{-1}$ );  $K$  is the Langmuir equilibrium parameter constant ( $\text{L mg}^{-1}$ );  $K_f$  is the adsorption capacity ( $\text{mg g}^{-1}$ ); and  $n$  is the Freundlich constant, a constant for a given system at a certain temperature, related to the physical properties and temperature of the adsorbent.

The adsorption kinetics were calculated using the following formula:

$$Q_t = Q_e(1 - e^{-k_1 t})$$

$$Q_t = \frac{Q_e^2 k_2 t}{1 + Q_e k_2 t}$$

where  $Q_t$  and  $Q_e$  ( $\text{mg g}^{-1}$ ) are the amounts of Cu adsorbed on biochar at time  $t$  and equilibrium, respectively; and  $k_1$  and  $k_2$  are the corresponding adsorption rate constants.

The soil was obtained from Yangzhou University agricultural experiment field, Yangzhou, China ( $119^\circ 23' \text{ E}$ ,  $32^\circ 20' \text{ N}$ ). The soil properties were as follows: pH, 7.75; organic matter,  $5.96 \text{ g kg}^{-1}$ ; total Cu,  $111.10 \text{ mg kg}^{-1}$ . 3 kg soil (of air-dry soil and sieved using a 2-mm sieve) were placed in plastic beaker.

Five treatments were prepared in triplicate as follows: control (CK), BC400, BC600, BC400-Cu and BC600-Cu. Except for CK, 2%(W/W) BC400, BC600, BC400-Cu and BC600-Cu were added into a plastic beaker. The mixture

was stirred to be well homogenized and then incubated at room temperature (25°C) for 30 days. Base fertilizer (N, 180 mg kg<sup>-1</sup>; P<sub>2</sub>O<sub>5</sub>, 90 mg kg<sup>-1</sup>; K<sub>2</sub>O, 120 mg kg<sup>-1</sup>) were mixed with the soil. Then, after sowing and thinning out seedlings of Ryegrass (*Lolium perenne* L.), 40 healthy individuals were kept in each pot. During the test, the weighing method was used to maintain the soil moisture content at about 60% of the saturated water-holding capacity. The ryegrass was grown for a total of 120 days, during which the above ground part biomass of the it was harvested once every 30 days for a total of four harvests. After each harvest, it was dried at 105°C for 0.5 h, 65°C for 24 h, and then weighed. Finally, the four harvested ryegrass samples were mixed and crushed to pass through a 0.90-mm sieve, then plant samples were carried out by dry ashing. The different fractions of Cu in the soil samples have been determined

by means of BCR sequential extraction method which was developed by the European Bureau of Reference. Cu was measured by inductively coupled plasma mass spectrometry (ICP-MS; Thermo Fisher Scientific, USA).

## Results and Discussion

The basic physical and chemical properties of BC400 and BC600 were shown in Table 1. The yield of the biochars decreased from 37.6% to 31.7% as the temperature increased from 400 to 600°C, the decrease yield of the biochars with temperature was similar to the reports by Zhu et al. (2018) which was attributed to the loss of volatiles and the condensation of aliphatic compounds because of increasing temperature. In addition, BC600 had a higher ash content compared to BC400. BC600 had a high pH and a low CEC value. Our results were consistent with the reported by Wang et al. (2013).

The atomic ratios of H/C, O/C and (N+O)/C of organic components in biochar could reflect the aromaticity, hydrophilicity and polarity of biochar samples. As the atomic ratio of H/C decreases, the degree of aromaticity increased, and as the ratio of O/C and (N+O)/C increased, the aromatic structure and polar groups also increased (Chi et al. 2017; Jung et al. 2013). Table 1 showed that the aromaticity and polarity of BC600 were greater than BC400, indicating that the former had more aromatic structures and polar groups. Chen et al. suggested that high temperatures were beneficial to the thermal transformation of organic matter into carbonized organic matter and the structure containing dense ring carbon (Chen et al. 2014). Surface area of the biochar increased from 13.07 to 29.00 m<sup>2</sup> g<sup>-1</sup> as temperature increases from 400 to 600°C (Table 1).

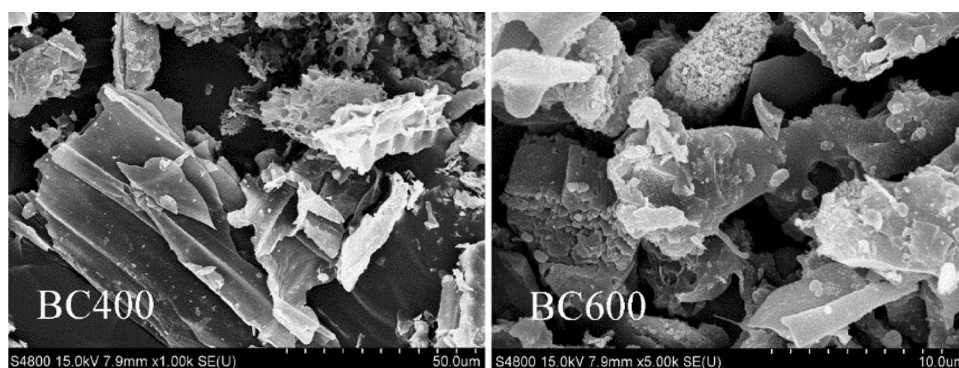
Figure 1 showed that BC400 were primarily strip-like, neatly arranged and had a smooth surface, whereas BC600 were more granular in appearance and had a rougher surface. Compared with BC400, pores on BC600 were well developed, and the pore distribution was relatively dense. Hence,

**Table 1** Material properties of BC400 and BC600

Parameter	BC400	BC600
Yield (% dry wt)	37.6	31.7
Ash content (% dry wt)	25.27	31.35
pH(1:2.5)	11.73	12.61
pH <sub>pzc</sub>	8.83	9.53
CEC(cmol/kg)	52.97	32.63
C (% dry wt)	54.92	59.56
H (% dry wt)	3.60	2.09
N (% dry wt)	1.30	1.00
O (% dry wt)	14.2	5.4
S (% dry wt)	0.71	0.60
Mg (% dry wt)	0.88	1.40
Si (% dry wt)	1.12	10.88
Molar H/C (% dry wt)	0.78	0.42
Molar O/C (% dry wt)	0.19	0.068
Molar (N+O)/C (% dry wt)	0.21	0.082
Specific surface area (m <sup>2</sup> g <sup>-1</sup> )	13.07	29.00
Pore volume(cm <sup>3</sup> g <sup>-1</sup> )	0.027	0.048
Pore diameter Dv (d)	3.34	17.08

$$O\% = 100\% - C\% - H\% - N\% - S\% - \text{Ash}\%$$

**Fig. 1** The SEM of surface structure of BC400 and BC600



it can be concluded that the surface structural changes in biochar are significantly influenced by pyrolysis temperature.

Corresponding pore size distribution curve of BC400 and BC600 are shown in Fig. 2a and b. The rice straw biochar prepared at 400 and 600°C belongs to the typical TYPE IV curve, which indicated that biochar contains mesoporous structure. BC600 contains more mesoporous structure and the specific surface area than BC400.

The infrared spectra showed in Fig. 3 that the surface of biochar contained oxygen-containing functional groups, such as  $-\text{COOH}$ ,  $-\text{OH}$ , aromatics, lipids, and alkane. The adsorption peaks near 3215 and 3366  $\text{cm}^{-1}$  are the stretching vibration peaks of  $-\text{OH}$ , while the adsorption peaks near 2913  $\text{cm}^{-1}$  are the stretching vibration peaks of  $-\text{CH}_2$  in alicyclic hydrocarbons or naphthenic hydrocarbons (Frost et al. 2015). However, BC600 did not contain this peak. The results show that the increase of pyrolysis temperature resulted in the loss of alkane groups; the adsorption peaks near 1701 and 1799  $\text{cm}^{-1}$  were  $\text{C}=\text{O}$  stretching vibration adsorption peaks of carboxylic acid, indicating the presence of acids; the peaks near 776 and 789  $\text{cm}^{-1}$  were  $\text{C}-\text{H}$  bending vibration adsorption peaks of aromatic rings; the peaks at 1455 and 1615  $\text{cm}^{-1}$  were  $\text{C}=\text{C}$  bending vibration peaks; and the peaks near 1320 and 1393  $\text{cm}^{-1}$  were  $\text{C}-\text{O}-\text{C}$  stretching peaks. The existence of shrinkage vibration peaks clearly shows the existence of benzene ring substances on the surface of biochar, indicating that rice straw formed a good aromatic structure during carbonization (Mohanty et al. 2013). In general, BC600 contained more aromatic structure substances than BC400.

Comparing the functional group compositions of biochars prepared at the two temperatures, which reveals that BC400 and BC600 have the same types of groups, similar characteristic adsorption peaks, and more

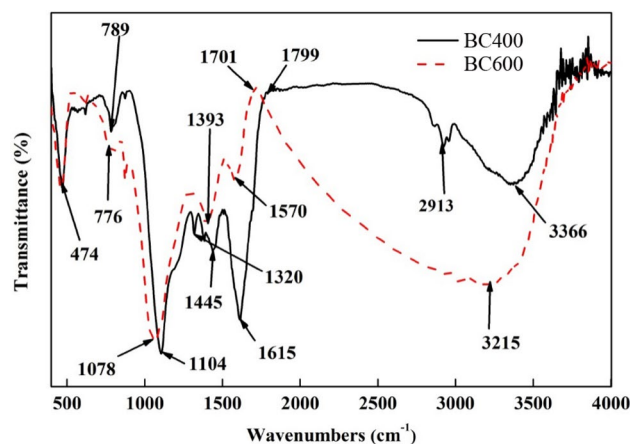


Fig. 3 FTIR spectra of BC400 and BC600

oxygen-containing functional groups such as  $-\text{COOH}$  and  $-\text{OH}$  on the surface, those cations have the ability of adsorbing. The primary variation between the two temperature biochars is shown in  $-\text{OH}$  and  $-\text{CH}_2$ . The vibration peak of  $-\text{OH}$  is weaker than the corresponding vibration peak of BC400, but it contains more aromatic structures, which is consistent with the results of surface element composition (Table 1). That is, with the increase of temperature, the degree of aromatization increases. According to Weidemann et al. (2017) the degree of aromatization of aromatic components increases with the increase of temperature at 400°C and above.

The parameters in Table 2 showed that the fitting degree between BC400 and BC600 for Cu adsorption and Langmuir adsorption model ( $R^2$  of 0.957 and 0.971, respectively) is better than that with the Freundlich adsorption model ( $R^2$  of 0.857 and 0.804, respectively). The results

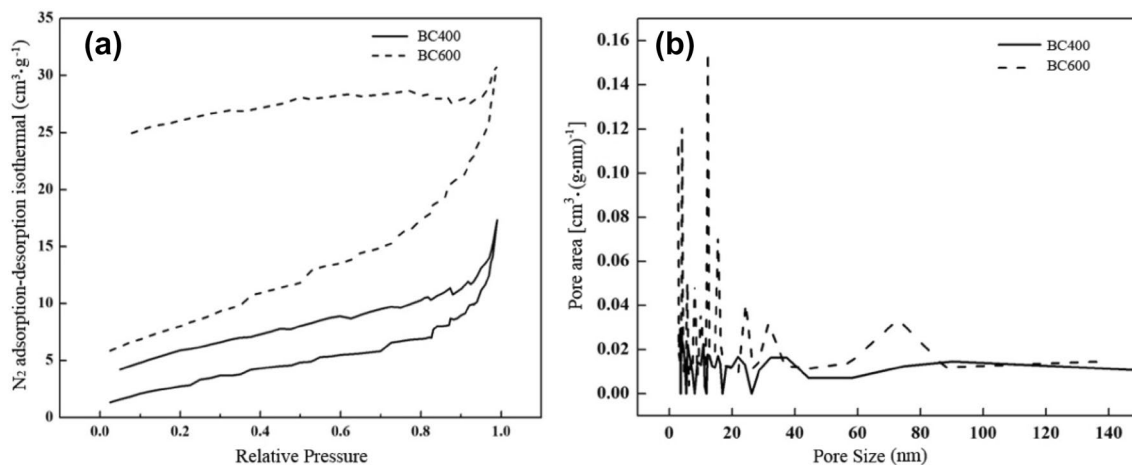
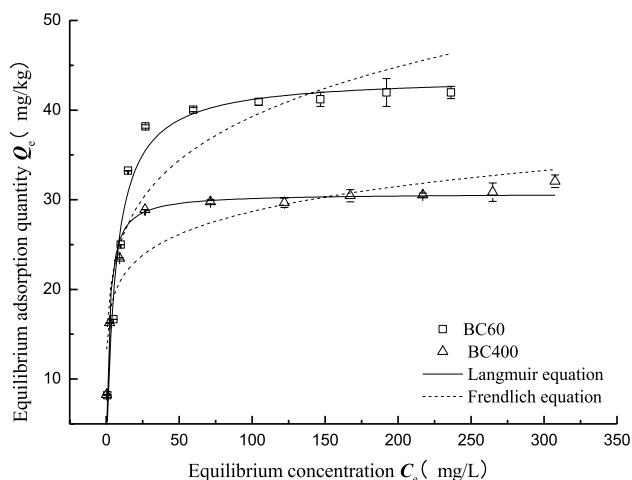


Fig. 2  $\text{N}_2$  adsorption–desorption isothermal **a** and Barrett–Joyner–Halenda (BJH) Corresponding pore size distribution curve **b** of BC400 and BC600

**Table 2** Parameters in the fitting model of Langmuir and Freundlich isothermal adsorption of  $\text{Cu}^{2+}$  on biochar surface

Biochars	Langmuir parameters			Freundlich parameters		
	$R^2$	$K$	$Q_m$	$R^2$	$K_f$	$n$
BC400	0.957	0.531	30.70	0.857	15.449	7.463
BC600	0.971	0.160	43.75	0.804	16.278	5.236

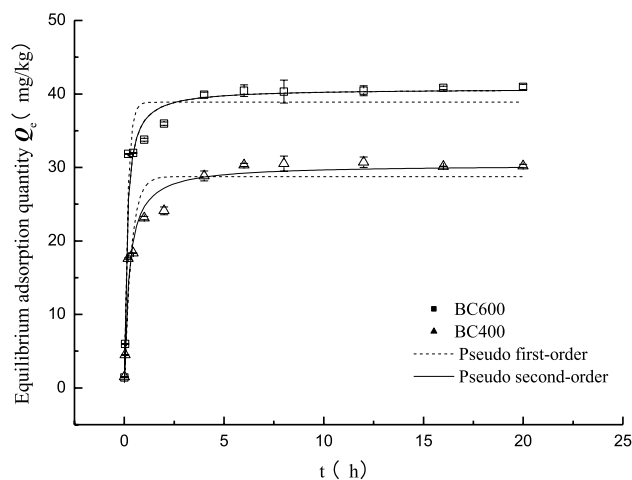
$$K = (\text{L mg}^{-1}), Q_m = (\text{g kg}^{-1}), K_f = (\text{g}^{1-n} \text{L}^n \text{kg}^{-1})$$

**Fig. 4** Langmuir and Freundlich adsorption isotherms for the adsorption of  $\text{Cu}^{2+}$  by biochar

reveal that the adsorption of Cu by BC400 and BC600 was mainly monolayer adsorption (Li et al. 2017) (Fig. 4).

Moreover, the maximum adsorption capacity of BC600 ( $Q_m = 43.75 \text{ mg g}^{-1}$ ) was higher than that of BC400 ( $Q_m = 30.70 \text{ mg g}^{-1}$ ), and the Cu adsorption capacity of BC600 was higher than that of BC400 in the Cu concentration range of 0–300  $\text{g kg}^{-1}$ .

The kinetic sorption data were described using the pseudo first-order and pseudo second-order models. The effect of transfer rate on Cu absorption by BC400 and BC600 was represented in Fig. 5. Table 3 showed the fitted model parameters for these models. The Cu sorption by BC400 and BC600 reached equilibrium after 4 h. The equilibrium adsorption capacity of BC600 was higher than that of BC400. Compared with the pseudo first-order kinetic model ( $R^2$  of 0.9215 and 0.94545, respectively), the kinetic process of Cu absorption by BC400 and BC600 was better fitted by the pseudo second-order kinetic model ( $R^2$  of 0.97075 and 0.95437, respectively), which was used to describe chemisorption (Ho and McKay 1999; Liu and Fan 2018; Wei et al. 2015). The pseudo second-order kinetic model fitted the sorption data with a higher consistency between theoretical and experimental  $Q_e$  values. The  $k_2$  value of BC600 was higher than that of BC400, indicating that the rate of Cu adsorbed by BC600 was faster than that adsorbed by BC400, which shows higher ash content, functional groups and pH

**Fig. 5** Adsorption kinetics for Cu adsorption by BC400 and BC600

of biochar contribute to the adsorption of Cu in aqueous solution (Sun et al. 2014).

Energy spectrum analysis of biochar surface elements can be used to indicate whether the biochar surface can adsorb heavy metals. The energy spectrum shown in Fig. 6 reveals that Cu was not detected on the surfaces of BC400 and BC600. The characteristic peaks of Cu appeared on the surfaces of BC400-Cu and BC600-Cu. This confirms that  $\text{Cu}^{2+}$  had been adsorbed on the surface of BC400 and BC600.

Figure 7 shows the effect of biochar on the Cu concentration of different fractions and pH values in soil. The pH values of the BC400 and BC600 treatment were significantly higher than CK (pH 8.57), increasing by 0.18 and 0.14 units, respectively. It has to do with that biochar have high alkalinity (Xu et al. 2016), the pH values of BC400 and BC600 is 11.73 and 12.61, respectively. The pH of biochar increases with the increase of pyrolysis temperature, this trend is consistent with many reported studies (Zhang et al. 2015). The mineral elements (K, Na, Ca, Mg, etc.) of biochar complexed with organic matter gradually, then changed to oxidation or phosphate state during pyrolysis, and the higher the pyrolysis temperature, the higher the content of inorganic mineral components (such as carbonate) (Yuan et al. 2011). While the pH values of the BC400-Cu and BC600-Cu treatments decreased, which were 8.31 and 8.29, respectively. Because of  $\text{CuSO}_4$  adsorbed by biochar, the pH values of BC400-Cu and BC600-Cu is low than BC400 and BC600.

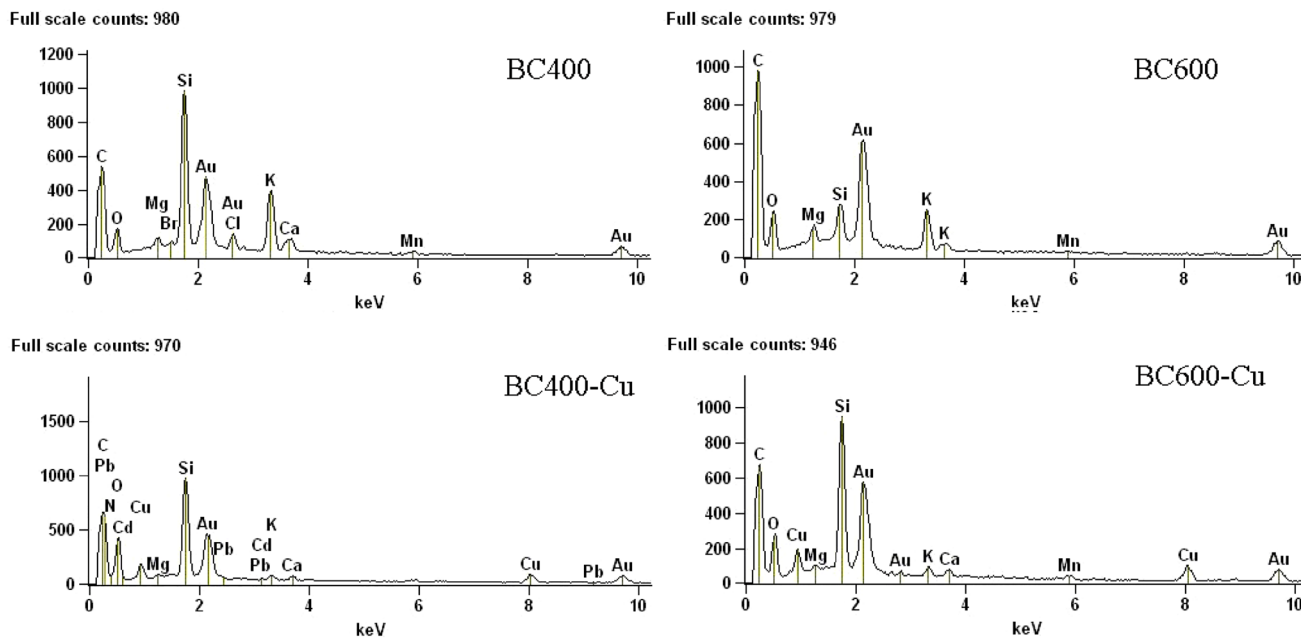


Fig. 6 EDS of BC400 and BC600

Table 3 Kinetic fitting parameters for Cu adsorption by BC400 and BC600

Biochars	Pseudo first-order			Pseudo second-order		
	$R^2$	$k_1$	$Q_e$	$R^2$	$k_2$	$Q_e$
BC400	0.9215	2.92867	28.76	0.97075	0.14189	30.35
BC600	0.94545	5.99847	38.88	0.95437	0.20163	40.71

$k_1 = h, Q_e = (g\ kg^{-1}), k_2 = (kg\ h^{-1}\ g^{-1}), Q_e = (g\ kg^{-1})$

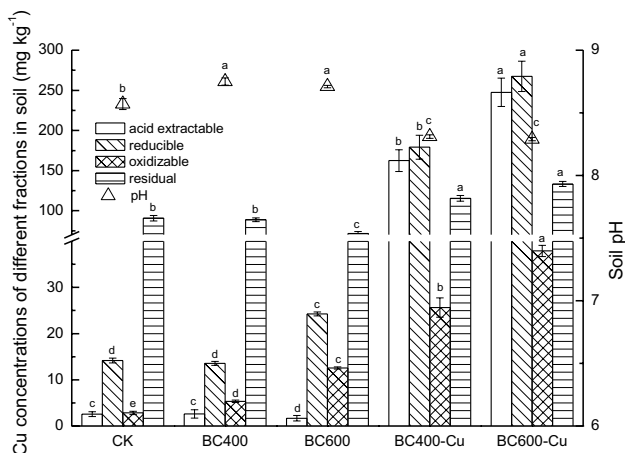
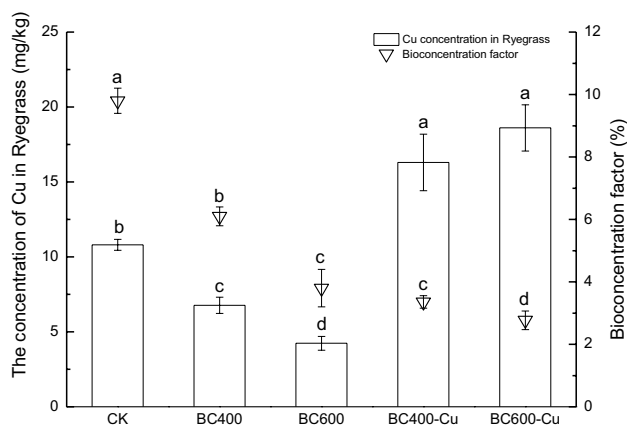


Fig. 7 Effect of different treatments on Cu concentrations of different fractions and pH in soils (mean ± SD, n = 3). Different letters above the blocks indicate significant differences ( $p < 0.05$ )

The toxicity of heavy metals in the soil environment is related not only to the total amount but also determined by the distribution of their fractions (Kabiri et al. 2019).

Different fractions produce different environmental effects, which directly affect the toxicity, migration and circulation of heavy metals. Acid extractable of heavy metal is absorbed the most easily, can better reflect the soil heavy metal biological effectiveness and mobility, through the determination of various forms of heavy metals in soil, especially the content of acid soluble state of heavy metal can be evaluation into the effect of improved material (Jamali et al. 2008). Figure 7. shows that the residual is mainly fraction of CK, the treatments of BC400 and BC600 in the soil and the acid extractable concentrations Cu in the treatment of BC600 significantly reduces, compare with CK. Due to the large specific surface area, pore structure and functional groups, biochar can adsorb heavy metals or form metal complexes with them (Dong et al. 2013), and Cd is gradually transferred from a more active form to a relatively stable form (Guo et al. 2017). The treatments of BC400-Cu and BC600-Cu are mainly in acid-soluble and reducible states, mainly because  $CuSO_4$  adsorbed by biochar enters the soil.

Cu concentration in ryegrass is shown in Fig. 8. Compared with  $10.80\ mg\ kg^{-1}$  of CK, Cu concentration in ryegrass of the BC400 and BC600 treatments decreased



**Fig. 8** Cu concentration in ryegrass and the bioconcentration factor of Cu (mean  $\pm$  SD,  $n=3$ ). Different letters above the blocks indicate significant differences ( $p < 0.05$ )

significantly, which were  $6.77$  and  $4.24 \text{ mg kg}^{-1}$ , respectively. This shows that biochar has a “passivation” effect on Cu in the soil, and reduces the absorption of Cu by ryegrass, and BC600 had a more passivation ability than BC400. Studies have shown that biochar can reduce bio-accessibility of Cu (Li et al. 2020) and the content of Cd in rice and available Cd in soil decreased gradually with the increase of biochar application (Chen et al. 2016). The treatments of BC400-Cu and BC600-Cu are treated by absorbing Cu and have two sources of Cu, one being soil Cu and the other is Cu absorbed by biochars. Compared with the BC400 and BC600 treatments, the average concentration of Cu ( $16.30$  and  $18.60 \text{ mg kg}^{-1}$ , respectively) in ryegrass increased significantly because of the abundant sources of Cu.

The ratio of Cu concentration in ryegrass to in soil was defined as the bioconcentration factor of Cu. The bioconcentration factor in CK was significantly higher than that of the BC400 and BC600 treatments. The results confirm that biochar can reduce the bioconcentration factor. Some studies indicate that when 1.5% bamboo biochar was applied to Cd-contaminated soil while growing pakchoi and maize, the bioavailability of cadmium was significantly reduced by 60.64% and 64.04%, respectively (Mohamed 2015). For the BC400-Cu and BC600-Cu treatments, the uptake of Cu by ryegrass can be attributed not only to soil Cu, but also to Cu absorbed by biochar. Although Cu concentration in ryegrass increased (Fig. 8), the bioconcentration factor of the BC400-Cu and BC600-Cu treatments was significantly lower than that of the BC400 and BC600 treatments, respectively, indicating that the release of Cu adsorbed by BC400 and BC600 in soil was greatly limited, and BC600 has comparatively stronger passivation than BC400.

Biochars produced from rice straw at two pyrolysis temperatures exhibited variable characteristics and efficiency towards Cu immobilization in the contaminated soils. This

study demonstrated that BC600 and BC400 have more aromatic and polar groups than BC400. The adsorption curves of BC400 and BC600 were more suited to the Langmuir isothermal adsorption model than the Freundlich model, indicating that the Cu adsorption is mainly monolayer. The saturated theoretical adsorption capacity of BC600 for  $\text{Cu}^{2+}$  can reach  $43.75 \text{ mg g}^{-1}$ . Kinetic analyses implied that the adsorption fitted well with pseudo-second-order model.

Moreover, the pot experiment shown that BC400 and BC600 not only have strong “passivation” effect on Cu in soil but also prevents the release of adsorbed Cu. The existence of these two effects can greatly reduce the bioconcentration factor. Due to the more aromatic polar groups, and higher pH, the passivation and release inhibition of BC600 are comparatively stronger than those of BC400. Therefore, the application of BC600 may be effective to reduce Cu pollution in Cu-contaminated soil.

**Acknowledgements** The authors acknowledge the financial supports from the National Natural Science Foundation of China (41471236), the Agricultural Science and Technology Innovation Fund of Jiangsu Province, China (CX(20)3082).

## References

- Akcil A, Erust C, Ozdemiroglu S, Fonti V, Beolchini F (2015) A review of approaches and techniques used in aquatic contaminated sediments: metal removal and stabilization by chemical and biotechnological processes. *J Clean Prod* 86:24–36. <https://doi.org/10.1016/j.jclepro.2014.08.009>
- Arakaki LNH, da Fonseca MG, da Silva Filho EC, de Alves M, de Sousa AP, Silva ALP (2006) Extraction of Pb(II), Cd(II), and Hg(II) from aqueous solution by nitrogen and thiol functionality grafted to silica gel measured by calorimetry. *Thermochim Acta* 450:12–15. <https://doi.org/10.1016/j.tca.2006.06.012>
- Brewer CE, Chuang VJ, Masiello CA, Gonnermann H, Gao X, Dugan B, Driver LE, Panzacchi P, Zygourakis K, Davies CA (2014) New approaches to measuring biochar density and porosity. *Biomass Bioenergy* 66:176–185. <https://doi.org/10.1016/j.biombioe.2014.03.059>
- Chen CP, Cheng CH, Huang YH, Chen CT, Lai CM, Menyailo OV, Fan LJ, Yang YW (2014) Converting leguminous green manure into biochar: changes in chemical composition and C and N mineralization. *Geoderma* 232–234:581–588
- Chen L, He LY, Wang Q, Sheng XF (2016) Synergistic effects of plant growth-promoting neorhizobium huautlense T1-17 and immobilizers on the growth and heavy metal accumulation of edible tissues of hot pepper. *J Hazard Mater* 312:123–131. <https://doi.org/10.1016/j.jhazmat.2016.03.042>
- Chen D, Wang XB, Wang XL, Feng K, Su JC, Dong JN (2020) The mechanism of cadmium sorption by sulphur-modified wheat straw biochar and its application cadmium-contaminated soil. *Sci Total Environ* 714:136550. <https://doi.org/10.1016/j.scitotenv.2020.136550>
- Chi T, Zuo JN, Liu FL (2017) Performance and mechanism for cadmium and lead adsorption from water and soil by corn straw biochar. *Front Environ Sci Eng* 11:15. <https://doi.org/10.1007/s11783-017-0921-y>

- Dong XL, Ma LQ, Zhu YJ, Li YC, Gu BH (2013) Mechanistic investigation of mercury sorption by Brazilian pepper biochars of different pyrolytic temperatures based on X-ray photoelectron spectroscopy and flow calorimetry. *Environ Sci Technol* 47:12156–12164. <https://doi.org/10.1021/es4017816>
- Frost R, Lopez A, Scholz R (2015) A SEM, EDS and vibrational spectroscopic study of the tellurite mineral: sonoraite  $\text{Fe}^{3+}\text{Te}^{4+}\text{O}_3(\text{OH})\cdot\text{H}_2\text{O}$ . *Spectrochim Acta*. 147:225–229. <https://doi.org/10.1016/j.saa.2015.03.089>
- Gaskin JW, Steiner C, Harris K, Das KC, Bibens B (2008) Effect of low-temperature pyrolysis conditions on biochar for agricultural use. *Trans Asabe* 51:2061–2069
- Guo FY, Ding CF, Zhou ZG, Huang GX, Wang XX (2017) Effects of combined amendments on crop yield and cadmium uptake in two cadmium contaminated soils under rice–wheat rotation. *Ecotoxicol Environ Saf* 148:303–310. <https://doi.org/10.1016/j.ecoenv.2017.10.043>
- Haghtalab A, Nabipoor M, Farzad S (2012) Kinetic modeling of the Fischer–Tropsch synthesis in a slurry phase bubble column reactor using Langmuir–Freundlich isotherm. *Fuel Process Technol* 104:73–79. <https://doi.org/10.1016/j.fuproc.2011.07.005>
- He XY, Liu ZX, Niu WJ, Yang L, Zhou T, Qin D, Niu ZY, Yuan QX (2018) Effects of pyrolysis temperature on the physicochemical properties of gas and biochar obtained from pyrolysis of crop residues. *Energy* 143:746–756. <https://doi.org/10.1016/j.energy.2017.11.062>
- Ho YS, Mckay G (1999) Pseudo-second order model for sorption processes. *Process Biochem* 34:451–465
- Jamali M, Kazi T, Arain M, Afridi H, Jalbani N, Memon A, Shah A (2008) Heavy metals from soil and domestic sewage sludge and their transfer to Sorghum plants. *Environ Chem Lett* 5:209–218. <https://doi.org/10.1007/s10311-007-0101-6>
- Joseph U, Adegoke T, Erinle K, Ejoh O, Akande T, George O, Zhao CS, Wang HY (2019) Effect of biochar on soil structure and storage of soil organic carbon and nitrogen in the aggregate fractions of an albic soil. *Arch Agron Soil Sci*. <https://doi.org/10.1080/03650340.2019.1587412>
- Jung C, Park J, Lim K, Park S, Heo J, Her NG, Oh J, Yun S, Yoon Y (2013) Adsorption of selected endocrine disrupting compounds and pharmaceuticals on activated biochars. *J Hazard Mater*. <https://doi.org/10.1016/j.jhazmat.2013.10.033>
- Kabiri P, Motaghian H, Hosseinpour A (2019) Effects of walnut leaves biochars on lead and zinc fractionation and phytotoxicity in a naturally calcareous highly contaminated soil. *Water Air Soil Pollut* 230:263. <https://doi.org/10.1007/s11270-019-4316-5>
- Kim MJ, Kim SC, Chung S, Kim S, Yoon JW, Park YJ (2020) Exploring the role of copper and selenium in the maintenance of normal thyroid function among healthy Koreans. *J Trace Elem Med Biol* 61:126558. <https://doi.org/10.1016/j.jtemb.2020.126558>
- Li Y, Wang ZW, Xie XY, Zhu JM, Li RN, Qin TT (2017) Removal of norfloxacin from aqueous solution by clay-biochar composite prepared from potato stem and natural attapulgit. *Colloids Surf A* 514:126–136. <https://doi.org/10.1016/j.colsurfa.2016.11.064>
- Li L, Jia ZL, Ma H, Bao WY, Li YZ (2019) The effect of two different biochars on remediation of Cd-contaminated soil and Cd uptake by *Lolium perenne*. *Environ Geochem Health* 41(5):2067–2080
- Li Y, Wang XJ, Wang Y, Wang F, Xia SQ, Zhao JF (2020) Struvite-supported biochar composite effectively lowers Cu bio-availability and the abundance of antibiotic-resistance genes in soil. *Sci Total Environ* 724:138294. <https://doi.org/10.1016/j.scitotenv.2020.138294>
- Liu L, Fan SS (2018) Removal of cadmium in aqueous solution using wheat straw biochar: effect of minerals and mechanism. *Environ Sci Pollut Res* 25:8688–8700
- Medellin-Castillo NA, Leyva-Ramos R, Ocampo-Perez R, de la Cruz RFG, Aragon-Pina A, Martinez-Rosales JM, Guerrero-Coronado RM, Fuentes-Rubio L (2007) Adsorption of fluoride from water solution on bone char. *Ind Eng Chem Res* 46:9205–9212. <https://doi.org/10.1021/ie070023n>
- Meng J, Liang SJ, Tao MM, Liu XM, Brookes PC, Xu JM (2018) Chemical speciation and risk assessment of Cu and Zn in biochars derived from co-pyrolysis of pig manure with rice straw. *Chemosphere* 200:344–350. <https://doi.org/10.1016/j.chemosphere.2018.02.138>
- Mohamed I (2015) Ecological restoration of an acidic Cd contaminated soil using bamboo biochar application. *Ecol Eng* 84:67–76
- Mohanty P, Nanda S, Pant KK, Naik S, Kozinski JA, Dalai AK (2013) Evaluation of the physicochemical development of biochars obtained from pyrolysis of wheat straw, timothy grass and pine-wood: effects of heating rate. *J Anal Appl Pyrol* 104:485–493. <https://doi.org/10.1016/j.jaap.2013.05.022>
- Namgay T, Singh B, Singh BP (2010) Influence of biochar application to soil on the availability of As, Cd, Cu, Pb, and Zn to maize (*Zea mays* L.). *Aust J Soil Res* 48:638–647. <https://doi.org/10.1071/SR10049>
- Ndeddy Aka RJ, Babalola OO (2016) Effect of bacterial inoculation of strains of *Pseudomonas aeruginosa*, *Alcaligenes faecalis* and *Bacillus subtilis* on germination, growth and heavy metal (Cd, Cr, and Ni) uptake of *Brassica juncea*. *Int J Phytoremediat* 18:200–209. <https://doi.org/10.1080/15226514.2015.1073671>
- Rakhra G, Masih D, Vats A, Verma SK, Singh VK, Rana RT, Kirar V, Singh SN (2017) Effect of physical activity and age on plasma copper, zinc, iron, and magnesium concentration in physically active healthy males. *Nutrition* 43–44:75–82. <https://doi.org/10.1016/j.nut.2017.06.005>
- Rambabu K, Bharath G, Fawzi B, Sagadevan V, Monash P, Show PL (2019) Date pits activated carbon for divalent lead ions removal. *J Biosci Bioeng* 128:88–97. <https://doi.org/10.1016/j.jbiosc.2018.12.011>
- Rizwan M, Lin QM, Chen XJ, Li YY, Li GT, Zhao XR, Tian YF (2020) Synthesis, characterization and application of magnetic and acid modified biochars following alkaline pretreatment of rice and cotton straws. *Sci Total Environ* 714:136532. <https://doi.org/10.1016/j.scitotenv.2020.136532>
- Salam A, Shaheen SM, Bashir S, Khan I, Wang JX, Rinklebe J, Rehman FU, Hu HQ (2019) Rice straw- and rapeseed residue-derived biochars affect the geochemical fractions and phytoavailability of Cu and Pb to maize in a contaminated soil under different moisture content. *J Environ Manag* 237:5–14. <https://doi.org/10.1016/j.jenvman.2019.02.047>
- Shahid M, Dumat C, Khalid S, Niazi N, Antunes P (2016) Cadmium bioavailability, uptake, toxicity and detoxification in soil-plant system. *Reviews of environmental contamination and toxicology* (continuation of residue reviews). Springer, Cham
- Sun JK, Lian F, Liu ZQ, Zhu LY, Song ZG (2014) Biochars derived from various crop straws: characterization and Cd(II) removal potential. *Ecotoxicol Environ Saf* 106:226–231. <https://doi.org/10.1016/j.ecoenv.2014.04.042>
- Sun X, Zhong T, Zhang L, Zhang KS, Wu WX (2019) Reducing ammonia volatilization from paddy field with rice straw derived biochar. *Sci Total Environ* 660:512–518. <https://doi.org/10.1016/j.scitotenv.2018.12.450>
- Trakal L, Veselská V, Šafařík I, Vítková M, Čihálová S, Komárek M (2016) Lead and cadmium sorption mechanisms on magnetically modified biochars. *Bioresour Technol* 203:318–324. <https://doi.org/10.1016/j.biortech.2015.12.056>
- Uchimiya M, Klasson KT, Wartelle LH, Lima IM (2011) Influence of soil properties on heavy metal sequestration by biochar amendment: 1. Copper sorption isotherms and the release of cations. *Chemosphere* 82:1431–1437. <https://doi.org/10.1016/j.chemosphere.2010.11.050>



- Wang Y, Hu YT, Zhao X, Wang SQ, Xing GX (2013) Comparisons of biochar properties from wood material and crop residues at different temperatures and residence times. *Energy Fuels* 27:5890–5899. <https://doi.org/10.1021/ef400972z>
- Wei XU, Lan HC, Wang HJ, Liu HM, Jiuhui QU (2015) Comparing the adsorption behaviors of Cd, Cu and Pb from water onto Fe-Mn binary oxide, MnO<sub>2</sub> and FeOOH. *Front Environ Sci Eng* 9:385–393
- Weidemann E, Buss W, Masek O, Jansson S (2017) Influence of pyrolysis temperature and production unit on formation of selected PAHs, oxy-PAHs, N-PACs, PCDDs, and PCDFs in biochar-A screening study. *Environ Sci Pollut Res*. <https://doi.org/10.1007/s11356-017-0612-z>
- Xu P, Sun CX, Ye XZ, Xiao WD, Zhang Q, Wang Q (2016) The effect of biochar and crop straws on heavy metal bioavailability and plant accumulation in a Cd and Pb polluted soil. *Ecotoxicol Environ Saf* 132:94–100. <https://doi.org/10.1016/j.ecoenv.2016.05.031>
- Yuan JH, Xu RK, Zhang H (2011) The forms of alkalis in the biochar produced from crop residues at different temperatures. *Bioresour Technol* 102:3488–3497. <https://doi.org/10.1016/j.biortech.2010.11.018>
- Yuvaraj A, Thangaraj R, Karmegam N, Ravindran B, Chang SW, Awasthi MK, Kannan S (2021) Activation of biochar through exoenzymes prompted by earthworms for vermibiochar production: a viable resource recovery option for heavy metal contaminated soils and water. *Chemosphere* 278:130458. <https://doi.org/10.1016/j.chemosphere.2021.130458>
- Zhang J, Liu J, Liu R (2015) Effects of pyrolysis temperature and heating time on biochar obtained from the pyrolysis of straw and lignosulfonate. *Bioresour Technol* 176:288–291. <https://doi.org/10.1016/j.biortech.2014.11.011>
- Zhu L, Zhao N, Tong LH, Lv YZ (2018) Structural and adsorption characteristics of potassium carbonate activated biochar. *RSC Adv* 8:21012–21019. <https://doi.org/10.1039/c8ra03335h>

**Publisher's note** Springer Nature remains neutral with regard to jurisdictional claims in published maps and institutional affiliations.